Egypt.J.Chem. **Vol. 63**, No.2, pp.449-460 (2020)

Egyptian Journal of Chemistry
http://ejchem.journals.ekb.eg/

Chitosan/TiO_2 nanocomposites: Effect of microwave heating and solution mixing techniques on physical properties

Labiba I. Hussein[1*], Abdaleem H. Abdaleem[2], Mohamed S. A. Darwish[1], Mohamed H. Mostafa[1] and Moataz A. Elsawy[1]
[1]Egyptian Petroleum Research Institute, Nasr City 11727, Cairo and [2]Menofia University, 32511, Menofia, Egypt

CHITOSAN/titanium oxide nanocomposite (CS/TiO_2 nanocomposite) could be prepared by different physical and chemical methods for various applications. CS/TiO_2 nanocomposite has been chemically prepared via microwave heating technique and physically prepared through solution mixing method. Fourier-transform infrared spectroscopy (FT-IR), X-ray diffraction spectroscopy (XRD), transmission electron microscopy (TEM) and dynamic light scattering (DLS) were used as spectral tools to characterize the functionality, phase, morphology and particles size of the prepared nanocomposites, respectively. The thermal stability was investigated by the thermogravimetric analysis (TGA), while optical properties were studied using ultraviolet-visible spectroscopy (UV-vis).The results have confirmed that CS/TiO_2 nanocomposite was chemically and physically prepared via the outer sphere complexation and the electrostatic repulsion between chitosan and titanium oxide nanoparticles surface (TiO_2 NPs), respectively. The thermal stability was enhanced with nanocomposite prepared by chemical method when compared to that prepared by the physical method. In addition, a significant shift in the peak of the chemically prepared nanocomposite from the UV region to visible region was observed. This shift could be attributed to the surface modification of TiO_2 NPs by the chemical reaction.

Keywords: Chitosan, Titanium oxide nanoparticles, Microwave heating, Solution mixing, Optical properties.

Introduction

Chitosan (CS) is a linear polysaccharide polymer that can be obtained from alkaline deacetylation of chitin, which is the second most abundant natural polymer in the world after cellulose [1]. CS consists of D-glucosamine and N-acetyl-D-glucosamine units via β -1, 4 glycosidic linkages [2]. CS exhibits favourable properties such as abundant availability, biodegradability, biocompatibility, non-toxicity and antimicrobial activity. These properties make CS desirable for various applications including food industry [3], agriculture [4], biomedical applications [5], cosmetics [6] and waste water treatment [7]. CS has active amine and hydroxyl groups on its backbone which makes it able for modification to improve its properties or acquire new properties [8]. CS could be physically modified into various physical forms such as membranes, fibres and hydrogels [9] or chemically modified via a variety of routes like crosslinking and grafting to widen its application in many fields [10].

The modification of CS with metal oxide nanoparticles such as oxides of zinc, iron, copper and titanium has attained great attention in the last decades due to the great value added to its properties [11]. Titanium oxide nanoparticles (TiO_2 NPs) has been widely used in distinct fields such as sensors [12], photocatalysis [13], biomedical and pharmaceutical applications [14] as a result of its biocompatibility, photo activity, biocompatibility, low production cost and abundant availability [15].

***Correspondence to**: Labiba I. Hussein (E-mail: Labiba51@yahoo.com
Received 12/12/2019; Accepted 120/1/2020
IDO 10.21608/ejchem.2020.20908.2245

Recently, Chitosan/TiO_2 nanocomposite (CS/TiO_2 nanocomposite) has been widely used in various applications such as food packaging [16] and dye removal [17], depending on its antimicrobial and photo catalytic activity [18].

CS/TiO_2 nanocomposite film has been used for packaging red grapes film as a result of its efficient antimicrobial activity against four tested strains, i.e. *Staphylococcus aureus, Escherichia coli, Aspergillus niger* and *Candida albicans* [19]. CS/TiO_2 nanocomposite film with improved tensile strength and barrier properties has been applied in postharvest management of fresh produce as it could delay the ripening process and extend the storage life of the tomato fruit [16]. Gene Q. Blantocas et al prepared CS/TiO_2 composite as an antimicrobial agent against *Staphylococcus. Aureus* [20]. CS/TiO_2 nanocomposite was employed for imparting improved antibacterial and mechanical properties to cellulosic paper via surface coating as reported by Yanjun Tang et al [21].

CS/TiO_2 nanocomposite removed rhodamine B (RhB) and congo red (CR) dyes under visible light irradiation as reported by K.T. Karthikeyan et al [22]. A report by Saja S. Al-Taweela et al showed that CS/TiO_2 nanocomposite with ratio 1:2 (TiO_2-CS) exhibited the highest surface area and showed high activity towards removal of Direct Violet 51 from its aqueous solutions [23]. CS was used as immobilizing agent to increase the photo catalytic efficiency of TiO_2 against methyl orange and alizarin red s dye as reported by Dhanya Aa et al [17]. CS/TiO_2 nanohybrid removed 90% of methylene blue dye under UV-light illumination and exhibited antibacterial activity of 100 % within 24 h of treatment against *Escheraichia coli* [18]. TiO_2 NPs-bonded CS nanolayer has been prepared by Mohamed E. Mahmoud et al to remove trace concentrations of Cd(II) and Cu(II) ions [24]. CS/TiO_2 nanocomposite showed the strongest inhibition in growth of rice bacterial pathogen Xanthomonas oryzae pv. oryzae (Xoo)[25].

Various methods have been used to prepare CS/TiO_2 nanocomposite such as solution blending [23] and chemical precipitation method [18]. CS/TiO_2 nanocomposite spheres were prepared without using crosslinking agent for wastewater treatment as reported by Keng-Shiang Huang et al [26]. On the other hand, Mohamed E. Mahmoud et al used glutaraldehyde as a crosslinking agent for surface crosslinking of CS nanolayers with TiO_2 NPs by the aid of microwave heating [27]. Adib Razzaz et al prepared CS/TiO_2 nanofibrous by two techniques: coating method (in which TiO_2 NPs coated chitosan nanofibers) and entrapped method (electrospinning of CS/TiO_2 solutions) [28].

In this work, comparative study was carried out between CS/TiO_2 nanocomposites prepared physically by solution mixing method and chemically via microwave heating technique. The prepared CS/TiO_2 nanocomposites were characterized by transmission electron microscopy (TEM), Fourier-transform infrared spectroscopy (FT-IR), X-ray diffraction spectroscopy (XRD) and dynamic light scattering (DLS).The thermogravimetric analysis (TGA) was used to compare the thermal behaviour of the prepared nanocomposites by different methods with neat CS. The surface modification of TiO_2 NPs and its effect on their optical properties due to the chemical reaction and physical blending with CS was studied using ultraviolet-visible spectroscopy (UV-vis).

Materials and experiments

Materials

Chitosan (extracted from crab shells, degree of deacetylation: 85% -low molecular weight) was purchased from Marine chemicals, India. Titanium oxide nanopowder and glacial acetic acid were obtained from Sigma Aldrich, USA. Distilled water has been used to prepare all the solutions. All the chemicals were of analytical grade and were used as received.

Chemical preparation of CS/TiO_2 nanocomposite

The chemical reaction between CS and TiO_2 NPs was carried out via the use of domestic microwave oven as source of energy. 0.5 g of TiO_2 NPs was dispersed in 50 ml of distilled water (solution 1). 0.5 g of CS was dissolved in 50 ml of 1% glacial acetic acid solution (solution 2).The solution 1 was added to solution 2 and were mixed in quick fit bottomed round flask. The flask was inserted in the microwave oven adjusted for 800 watt power and 10 min time. At the end of the reaction, decantation and washing with distilled water were carried out to remove unreacted materials and obtain the product. The product was dried in vacuum oven till constant weight.

physical preparation of CS/TiO_2 nanocomposite

0.5 gm of CS was dissolved in 50 ml of 1% acetic acid solution (solution 1). 0.5 g of TiO_2 NPs was dispersed in 50 ml of distilled water (solution 2). The mixture solution of solution 1 and solution

2 were stirred in quick fit bottomed round flask for 30 minutes at room temperature. The mixture solution was taken in a syringe and added dropwise to the ammonium hydroxide solution where chitosan/TiO_2 nanocomposite is precipitated. The precipitated CS/TiO_2 nanocomposite was taken out of the solution and dried at room temperature.

Characterization techniques

FT-IR spectra of CS, TiO_2 NPs and CS/TiO_2 nanocomposites in the range (400 - 4000 cm^{-1}) were recorded by a Shimadzu FTIR – 4200 spectrophotometer using a disk of 200 mg as a reference. The XRD patterns of TiO_2 NPs, CS and CS/TiO_2 nanocomposites were investigated using a modern PAN analytical diffractometer, Xpert PRO model and Cu K-Alpha radiation (1.54060 Å) was used with the scanning rate of 0.02°/step and 2θ ranging from 4.01° to 69.99°. The TEM images of TiO_2 NPs and CS/TiO_2 nanocomposites were obtained using TEM-1230 with an accelerating voltage of 100 KV (JEOL Co., Japan).The average particles size and zeta potential of TiO_2 NPs and CS/TiO_2 nanocomposite were determined by dynamic light scattering (DLS) by using Malvern Zetasizer Nano (Malvern Instruments Ltd, Worcestershire, UK). The thermogravimetric analysis of CS and CS/TiO_2 nanocomposites was determined by SDT Q600 V20.9 Build 20thermal gravimetric under a heating rate of 10◦C/min. The optical properties were investigated by V-750 UV-Vis spectrophotometer.

Results and Discussions

Preparation of CS/TiO_2 nanocomposite

TiO_2 NPs in contact with water or aqueous solutions become hydrated and form a monolayer of surface hydroxyl groups which become protonated (as they receive protons) or deprotonated (as they release protons), depending on the solution pH. This amphoteric character allows TiO_2 NPs to develop electrical surface charges which depend mainly on the solution pH and their point of zero charge (PZC).The pH at zero point of charge is defined as the pH at which the sum of the all the surface positive charges balances the sum of all the surface negative charges. As shown in Fig.1, at solution pH values lower than that of pH at PZC, TiO_2 NPs surface has positive charge, whereas at solution pH values higher than pH at PZC, the surface of TiO_2 NPs becomes negatively charged. This is described by equations, (1) and (2) [29].

$$TiOH(surf)+H^{+}(aq)\leftrightarrow TiOH^{+2}(surf) \quad (pH<pH_{pzc}) \quad (1)$$

$$TiOH(surf)+OH-(aq)\leftrightarrow TiO^{-}(surf)+H2O \quad (pH>pH_{pzc}) \quad (2)$$

Chemical route

CS has reactive amine groups on its backbone which are protonated in acidic medium, resulting in positively charged CS [31]. As indicated in Fig.2a, CS/TiO_2 nanocomposite was chemically prepared via the outer sphere complexation between the positively charged chains of CS and the negatively charged surface of TiO_2 NPs [32,33].

Physical route

As showed in Fig.2b, a proper pH value below the pH at PZC of TiO_2 NPs and the pKa of CS will enable both the surface of TiO_2 NPs and the molecular chains of CS to be positively charged. Under the electrostatic repulsion forces between the nanoparticles and the polymer matrix, the flexible chains of CS molecules can be fully stretched out, resulting in dispersion of TiO_2 NPs in CS matrix [29].

Morphology

TEM was used to investigate the morphology of TiO_2 NPs and CS/TiO_2 composites as shown in Fig.3. As shown in Fig.3a, TiO_2 particles were found to be in the nanoscale. From Fig.3b, It can be seen that TiO_2 NPs are coated by CS, showing evidence for the possibility of the chemical reaction of CS on TiO_2 NPs surface. Fig.3c showed that TiO_2 NPs are dispersed in CS matrix, indicating the successful physical preparation of CS/TiO_2 nanocomposite.

Particle size and zeta potential

Fig.4 (a,b) present DLS of the particles size distribution of TiO_2 NPs and chemically prepared CS/TiO_2 nanocomposite. It was found that the average particles size of TiO_2 NPs and CS/TiO_2 nanocomposite prepared by chemical method were 60 nm and 85 nm, respectively. The increased average particles size of chemically prepared CS/TiO_2 nanocomposite compared to TiO_2 NPs shows the existence of polymer structure on TiO_2 NPs. Fig.5 (a,b) indicate the zeta potential of TiO_2 NPs and CS/TiO_2 nanocomposite prepared by chemical method. The zeta potential of TiO_2 NPs was found to be - 21.6 mV as the pH of dispersion medium (distilled water) is higher than that pH at PZC of TiO_2 NPs [29]. It was found that the zeta potential of TiO_2 NPs was shifted to +2.73 mV after the chemical reaction with CS. The significant change in zeta potential value could be owing to the consumption of TiO_2 NPs active sites via their chemical reaction with CS in the chemically prepared CS/TiO_2 nanocomposite [34].

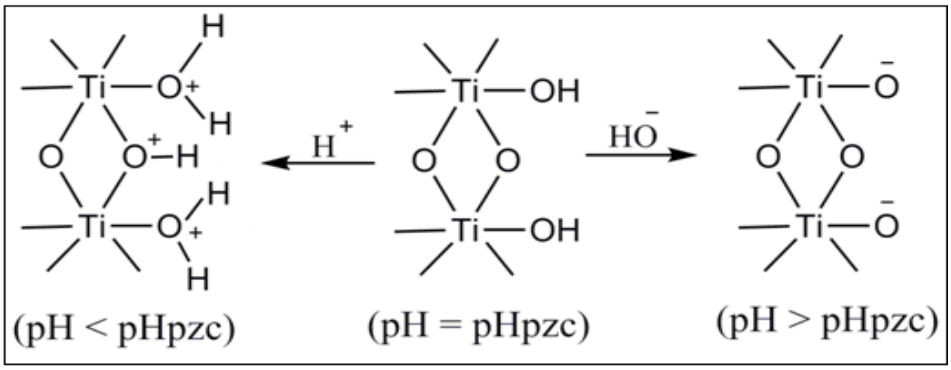

Fig.1. Simplified scheme of the protonation and deprotonation of hydroxylated TiO_2 surface leading to positive and negative net charge at the surface, respectively [30].

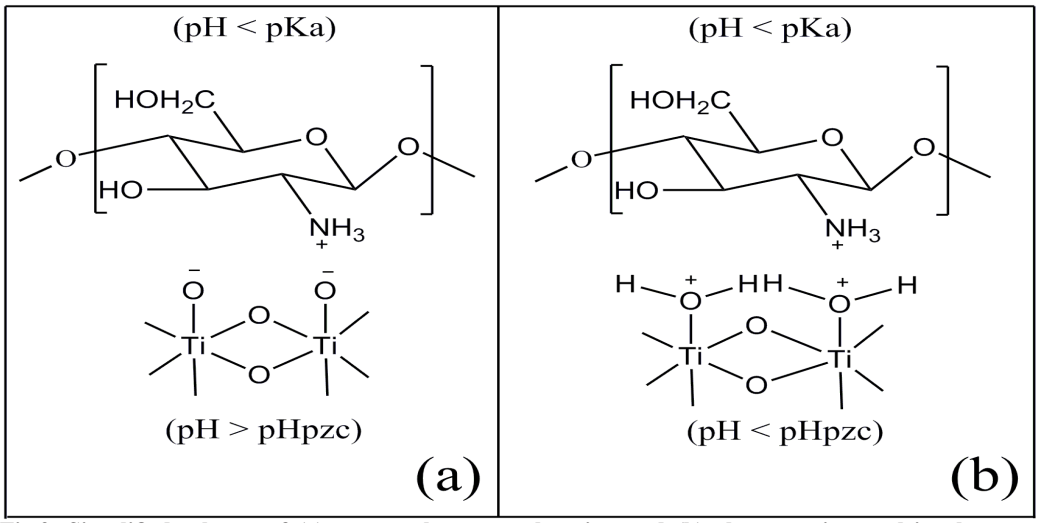

Fig.2. Simplified scheme of (a) outer sphere complexation and (b) electrostatic repulsion between charged CS chains and charged surface of TiO_2 NPs.

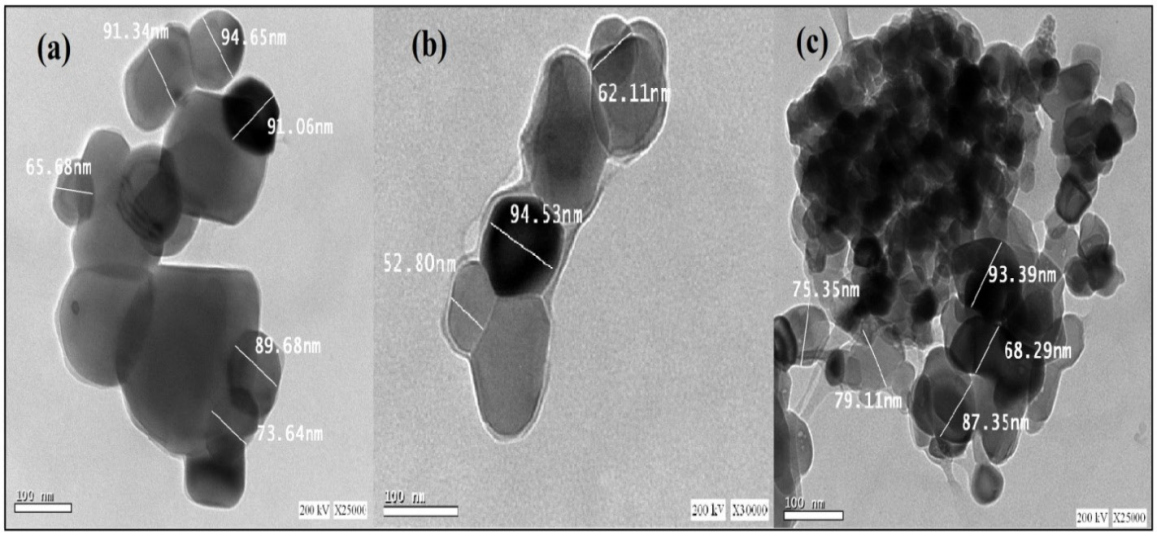

Fig.3.TEM images of (a) TiO_2 NPs, (b) chemically prepared CS/TiO_2 nanocomposite and (c) physically prepared CS/TiO_2 nanocomposite

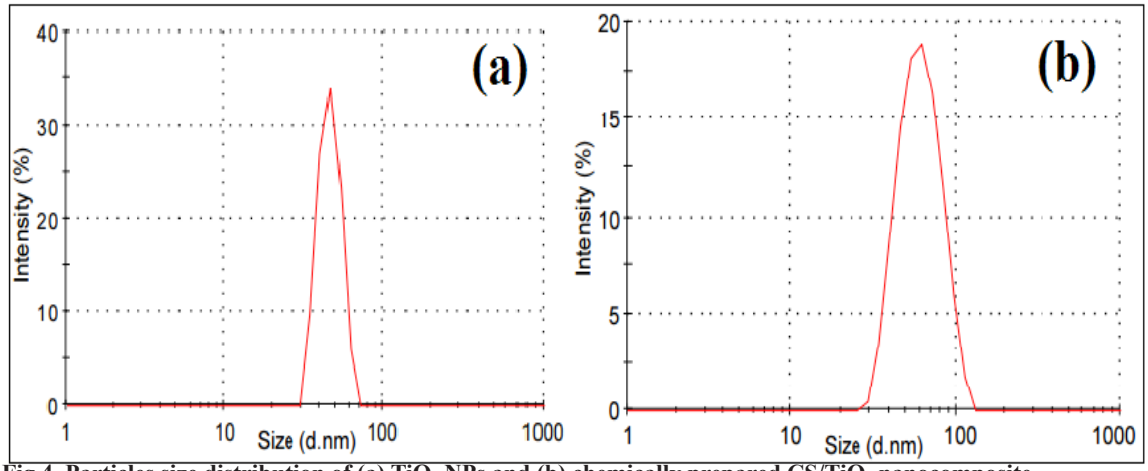

Fig.4. Particles size distribution of (a) TiO_2 NPs and (b) chemically prepared CS/TiO_2 nanocomposite.

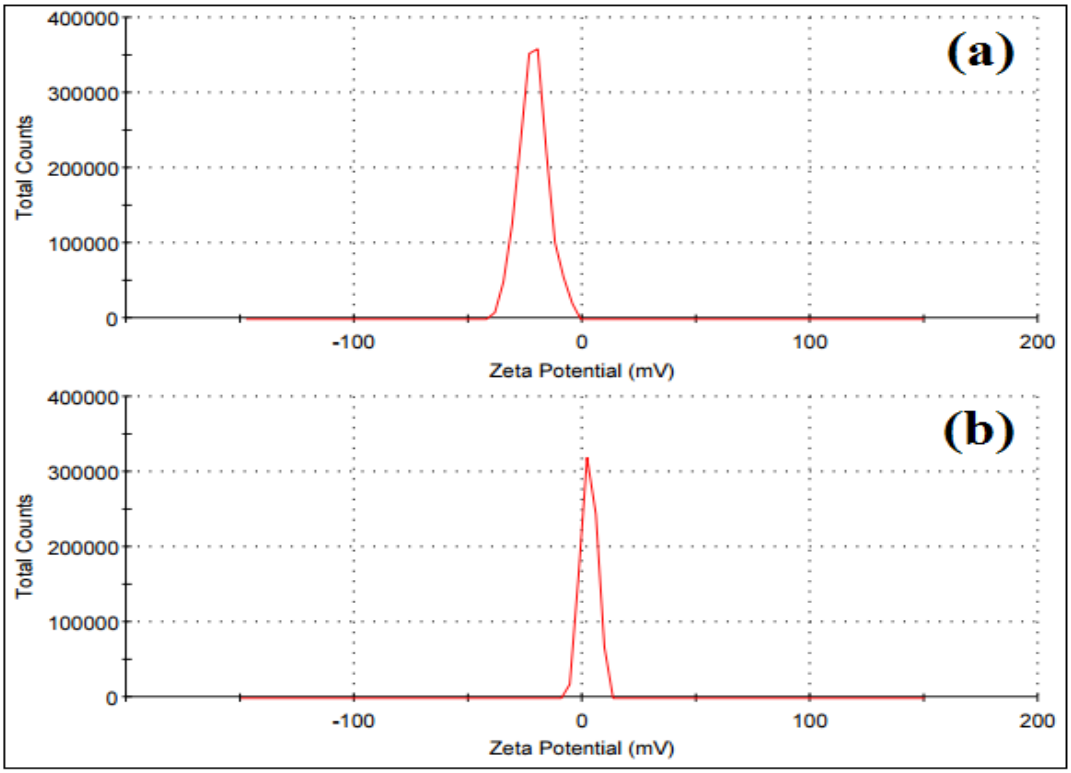

Fig.5. Zeta potential of (a) TiO_2 NPs and (b) chemically prepared CS/TiO_2 nanocomposite.

FT-IR spectroscopy

The FT-IR spectra of neat CS, TiO_2 NPs, chemically and physically prepared CS/TiO_2 nanocomposites are presented in Fig.6. TiO_2 NPs exhibited band at 499 cm^{-1} which corresponds to the stretching vibration of Ti-O as shown in Fig.6a.

From Fig.6b, neat CS exhibited band at 3365 cm^{-1} that could be attributed to the stretching vibrations of –OH and –NH_2 groups. The presence of band at 2877 cm^{-1} corresponds to the asymmetric stretching vibration of –CH group. The band at 1654 cm^{-1} was due to –C=O stretching (amide I). Appearance of band at1587 cm^{-1} was owing to N–H bending (amide II). Deformation of O-H and stretching of alcoholic group (CH_2-OH) are responsible for the bands at 1423 cm^{-1} and1380 cm^{-1} respectively. The bands at 1154 cm^{-1} and 1076

cm^{-1} were assigned to β (1-4) glycosidic bond in polysaccharide unit and the stretching vibration of C-O-C, respectively [35].

The FT-IR spectra of the chemically and physically prepared CS/TiO_2 nanocomposites are shown in Fig.6(c,d). Compared to neat CS, both chemically and physically prepared nanocomposite exhibited the characteristic peaks of both CS and TiO_2 NPs. However, the peaks assigned to the stretching vibration of OH and NH_2 groups were shifted to lower and higher wave numbers at 3055 cm^{-1} and 3428 cm^{-1} for the chemically and physically prepared nanocomposites, respectively. The shift to lower wave number in the chemically prepared nanocomposite could be due to the complexation between the opposite charges of CS and TiO_2 NPs surface. However, the shift to higher wave number in the physically prepared nanocomposite could be a result of the miscibility between the functional groups present on TiO_2 NPs surface and those of CS [36].

XRD spectrometry

Fig.7a represents the XRD pattern of CS that possesses broad peak at 20.36◦ which shows the semicrystalline nature of CS. The XRD pattern of TiO_2 NPs is displayed in Fig.7b with sharp peaks observed at 25.3◦, 37.9°, 48.4°, 55.3°, 63°and 69° which correspond to different diffraction planes of TiO_2 [37].

The XRD patterns of the chemically and physically prepared CS/TiO_2 nanocomposites shown in Fig.7c and Fig.7d, respectively exhibit the characteristic peaks of both TiO_2 NPs and CS. However, the prepared nanocomposites showed changes in intensity and sharpness of the characteristic peaks of CS and TiO_2 NPs, indicating that both CS and TiO_2 affect the crystallinity of each other.

Compared to CS, the obvious changes in intensity and sharpness in the nanocomposite prepared by chemical method could be considered as an evidence for the chemical reaction of CS on TiO_2 NPs surface.

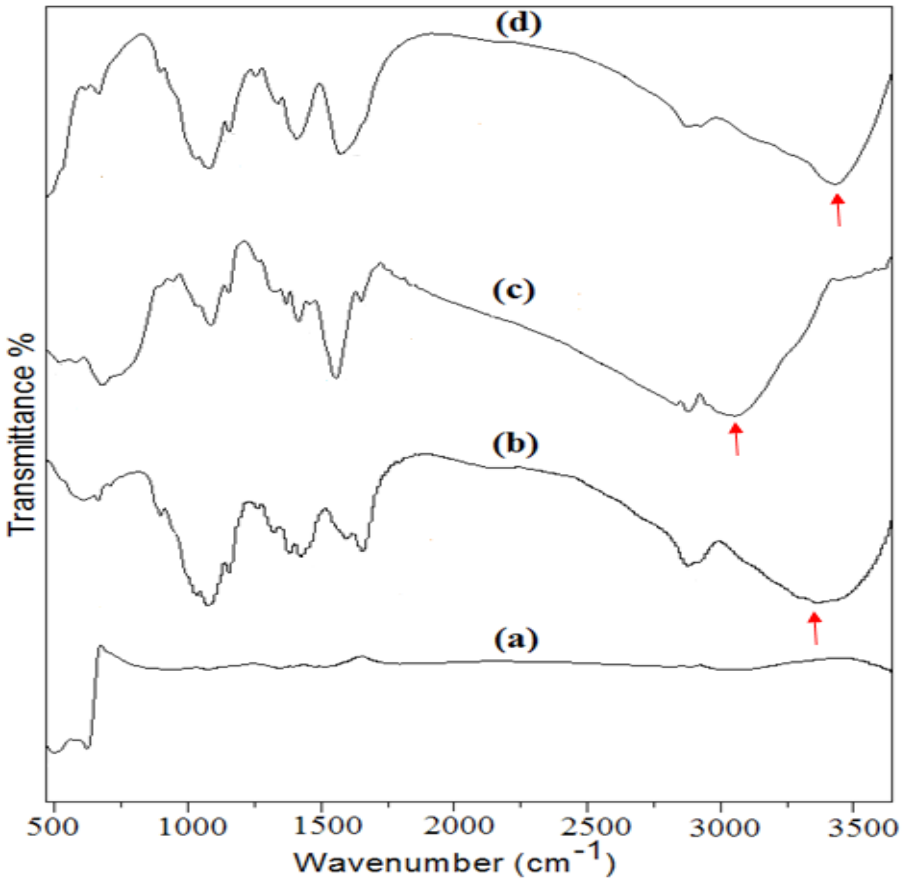

Fig.6. FT-IR spectra of TiO_2 NPs (a), CS(b), the chemically prepared CS/TiO_2 nanocomposite (c) and the physically prepared CS/TiO_2 (d).

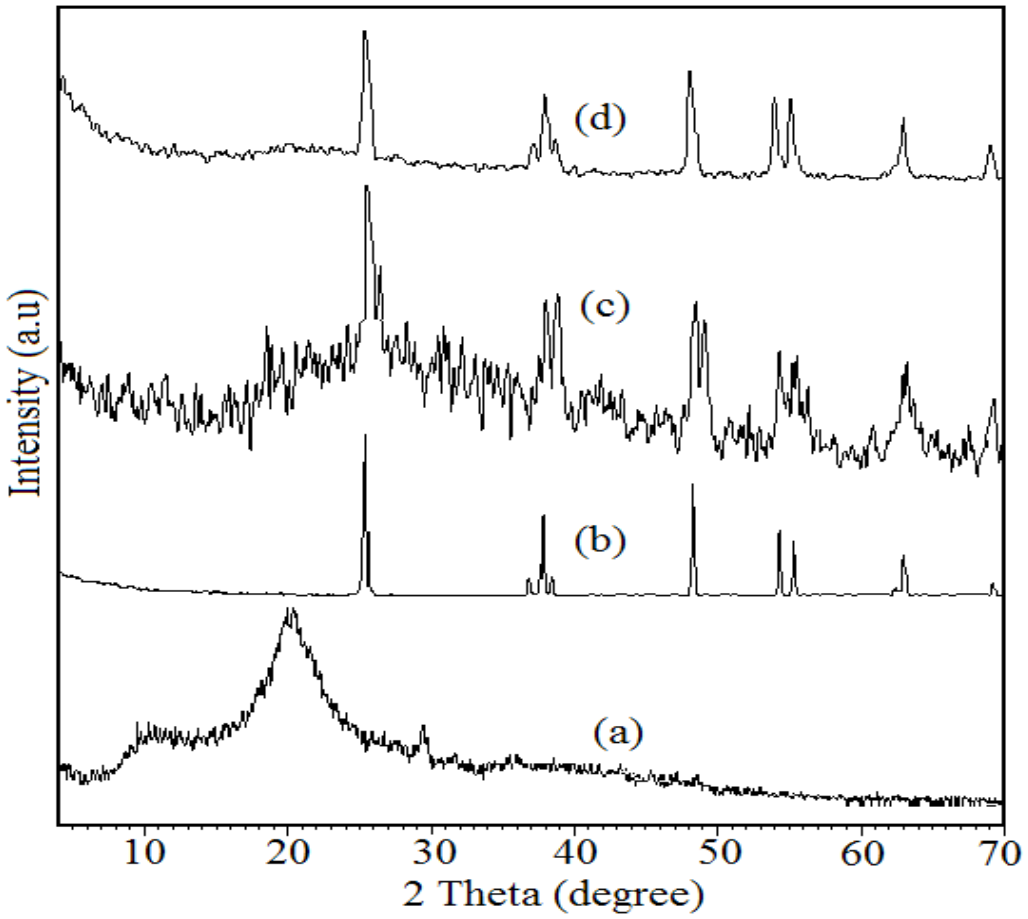

Fig.7. XRD patterns of CS (a), TiO_2 NPs (b), chemically prepared CS/TiO_2 nanocomposite (c) and physically prepared CS/TiO_2nanocomposite (d).

The thermal behaviour of CS, chemically and physically prepared CS/TiO_2 nanocomposites was studied by TGA as presented in Fig.8. It was found that the prepared CS/TiO_2 nanocomposites exhibit significant enhancement in the thermal stability compared to CS. Additionally, the nanocomposite prepared by chemical method was more thermally stable when compared to that prepared by the physical method. The chemically and physically prepared nanocomposites possess onset decomposition temperatures at 274°C and 251°C, respectively that are higher than that of CS (235°C). The temperatures at maximum decomposition of CS, chemically and physically prepared nanocomposites were 240°C, 291°C and 273°C, respectively. Moreover, the decomposition of CS and nanocomposites at 100 °C was attributed to water removal. From the results, it could be seen that the chemical type of nanocomposite showed higher thermal stability than both CS and the physical type of nanocomposite. This behaviour may be attributed to the chemical bond between CS and TiO_2 NPs enhanced the overall bonds strength of CS/TiO_2 nanocomposite which is confirmed by the strong shift of IR peaks compared to CS and physical nanocomposite. The residual mass percentages which result from decomposition of CS, physically and chemically prepared nanocomposites at 700°C were 48%, 55% and 60% respectively. These data show that by increasing temperature, the prepared nanocomposites exhibited higher residual mass percentages compared to CS. This behaviour could be a result of the presence of TiO_2 NPs in CS/TiO_2 nanocomposites.

UV-Visible spectroscopy

TiO_2 can be recognized as a semiconductor that possesses wide band gap energy. The electron transfer from valence band to conductive band reveals significant absorption peak [38]. The UV-Vis absorbance spectra of CS, TiO_2 NPs, the physically and the chemically

prepared CS/TiO_2 nanocomposites are presented in Fig.9. TiO_2 NPs exhibits absorption peak at 377 nm, while that of physically and chemically prepared CS/TiO_2 nanocomposites were found to be at 382 nm and 404 nm, respectively. It can be seen that the physically prepared nanocomposite exhibits absorption peak in the UV region which is the same behaviour of TiO_2 NPS. In the nanocomposite prepared chemically, the absorption peak was showed up in the visible region which can be attributed to the surface modification of TiO_2 NPs, caused by the chemical reaction of CS on TiO_2 NPs surface. This in turn reduces the band gap energy of TiO_2 NPs, enabling the photo catalytic reactions to take place in the visible light range. Consequently, the photo catalytic activity of TiO_2 NPs was enhanced in terms of absorption of more photons and saving energy compared to TiO_2 NPs itself [39].

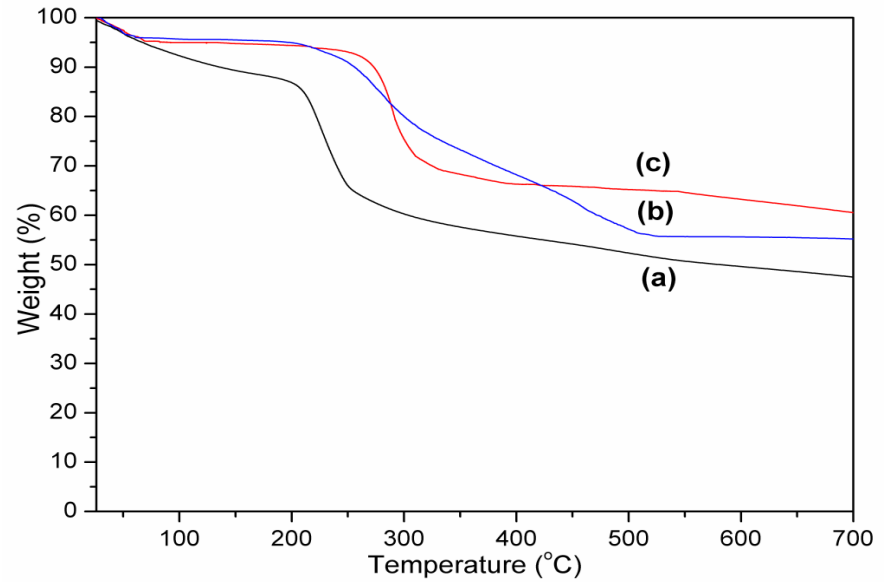

Fig.8. TGA curves of CS (a), physically prepared CS/TiO_2 nanocomposite (b) and chemically prepared CS/TiO_2 nanocomposite (c).

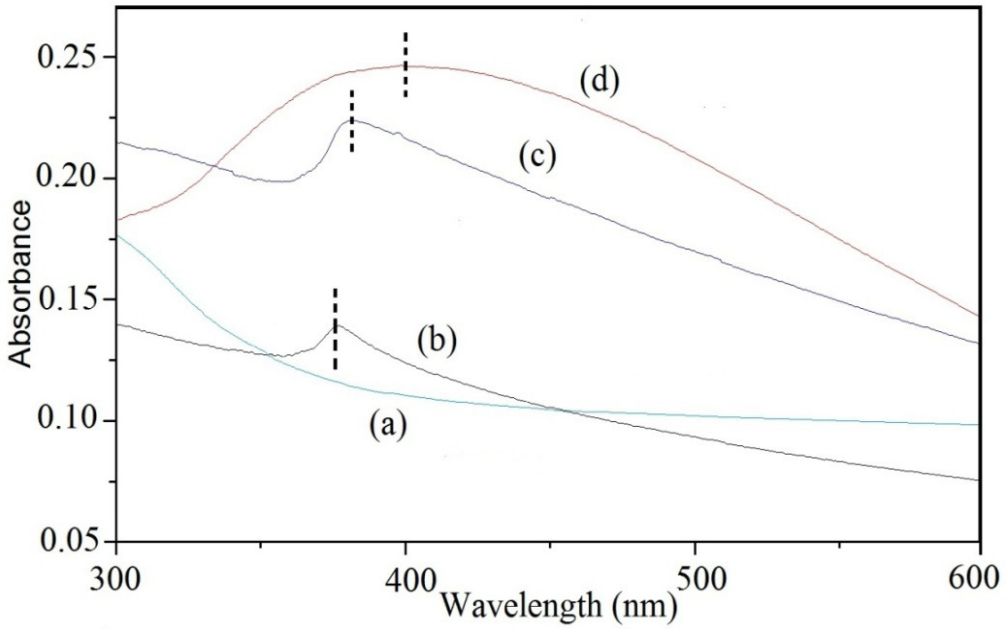

Fig.9. UV-Visible spectra of CS (a), TiO_2 NPs (b), the physically prepared CS/TiO_2 nanocomposite (c) and the chemically prepared CS/TiO_2 (d) .

Conclusion

CS/TiO_2 nanocomposite has been physically and chemically prepared as indicated from the FT-IR, XRD, TEM and DLS results. CS/TiO_2 nanocomposite was chemically prepared via outer sphere complexation of the opposite charges of CS chains and TiO_2 NPs surface using microwave heating technique. The physical preparation of CS/TiO_2 nanocomposite was carried out through the electrostatic repulsion of CS chains and surface of TiO_2 NPs, resulting in stretching out of CS chains and improved dispersion of TiO_2 NPs in CS matrix. The TGA results showed that the chemically prepared CS/TiO_2 nanocomposite was more thermally stable relative to the nanocomposite prepared by physical method. The UV-Vis studies showed that the physically prepared nanocomposite exhibits absorption peak in the UV region which is the same behaviour of TiO_2 NPs. However, the surface modification of TiO_2 NPs by their chemical reaction with CS enabled the photo catalytic reactions to take place in the visible light range, resulting in absorption of more photons and saving energy compared to TiO_2 NPs itself.

References

1. Abdel-Zaher N. A., El-Bassyouni G. T., Moselhey M. T. and Guirguis O. W., Structural, Thermal and Optical Modifications of Chitosan due to UV-Ozone Irradiation. *Egypt. J. Chem.*, **61,** 447-460 (2018).
2. Kyzas G. Z. and Bikiaris D. N. , Recent modifications of chitosan for adsorption applications: A critical and systematic review. *Mar. Drugs*, **13,** 312–337 (2015).
3. Wang H., Qian J. and Ding F. , Emerging chitosan-based films for food packaging applications. *J. Agric. Food Chem.*, **66,** 395–413 (2018).
4. Malerba M. and Cerana R. , Recent advances of chitosan applications in plants. *Polymers (Basel).*, **10,** 118 (2018).
5. Zhao D., Yu S., Sun B., Gao S., *et al.* , Biomedical applications of chitosan and its derivative nanoparticles. *Polymers (Basel).*, **10,** 462 (2018).
6. Aranaz I., Acosta N., Civera C., Elorza B., *et al.* , Cosmetics and cosmeceutical applications of chitin, chitosan and their derivatives. *Polymers (Basel).*, **10,** 213 (2018).
7. Muxika A., Etxabide A., Uranga J., Guerrero P. and Caba K . De. , Chitosan as a bioactive polymer : Processing , properties and applications. *Int. J. Biol. Macromol.*, **105,** 1358–1368 (2017).
8. Mahmoud G. M., Abdel Khalek M. A., Shoukry E. M., Amin M. and Abdulghany A. H., Removal of Phosphate Ions from Wastewater by Treated Hydrogel Based on Chitosan. *Egypt. J. Chem.*, **62,** 1537-1549 (2019).
9. Moura J. M., Gründmann D. D. R., Cadaval T. R. S., Dotto G. L. and Pinto L. A. A., Comparison of chitosan with different physical forms to remove Reactive Black 5 from aqueous solutions. *J.Environ.Chem.Eng.*, **4,** 2259–2267 (2016).
10. Taher M. A., Omer A. M., Hamed A. M., Ali A. M., Tamer T. M. and Mohy Eldin M. S., Development of Smart Alginate/chitosan Grafted Microcapsules for Colon Site-specific Drug Delivery. *Egypt. J. Chem.*, **62,** 1037-1045 (2019).
11. Sunil D. , Recennt advances on Chitosan-Metal Oxide Nanoparticles and their biological Application. *Materials Science Forum***754,** 99–108 (Trans Tech Publ, 2013).
12. Bai J. and Zhou B. , Titanium dioxide nanomaterials for sensor applications. *Chem. Rev.*, **114,** 10131–10176 (2014).
13. Khairy M. and Zakaria W. , Effect of metal-doping of TiO2 nanoparticles on their photocatalytic activities toward removal of organic dyes. *Egypt. J. Pet.*, **23,** 419–426 (2014).
14. Çeşmeli S. and Biray Avci C. , Application of titanium dioxide (TiO2) nanoparticles in cancer therapies. *J. Drug Target.*, **27,** 762–766 (2019).
15. Nadeem M., Tungmunnithum D., Hano C., Abbasi B. H., et al. , The current trends in the green syntheses of titanium oxide nanoparticles and their applications. *Green Chem. Lett. Rev.*, **11,** 492–502 (2018).
16. Kaewklin P., Siripatrawan U., Suwanagul A. and Lee Y. S. , Active packaging from chitosan-titanium dioxide nanocomposite film for prolonging storage life of tomato fruit. *Int. J. Biol. Macromol.*, **112,** 523–529 (2018).
17. Dhanya A. and Aparna K . , Synthesis and Evaluation of TiO2/Chitosan Based Hydrogel for the Adsorptional Photocatalytic Degradation of Azo and Anthraquinone Dye under UV Light Irradiation. *Procedia Technol.*, **24,** 611–618 (2016).

18. Haldorai Y. and Shim J. , Novel chitosan-TiO2 nanohybrid: Preparation, characterization, antibacterial, and photocatalytic properties. *Polym. Compos.*, **35,** 327–333 (2014).

19. Zhang X., Xiao G., Wang Y., Zhao Y., *et al.* , Preparation of chitosan-TiO2 composite film with efficient antimicrobial activities under visible light for food packaging applications. *Carbohydr. Polym.*, **169,** 101–107 (2017).

20. Blantocas G. Q., Alaboodi A. S. and Abdel-baset H. M. , Synthesis of Chitosan – TiO2 Antimicrobial Composites via a 2-Step Process of Synthesis of Chitosan – TiO 2 Antimicrobial Composites via a 2-Step Process of Electrospinning and Plasma Sputtering. *Arab. J. Sci. Eng.*, **43,** 389–398 (2018).

21. Tang Y., Hu X., Zhang X., Guo D., *et al.* , Chitosan/ titanium dioxide nanocomposite coatings: Rheological behavior and surface application to cellulosic paper. *Carbohydr. Polym.*, **151,** 752–759 (2016).

22. Karthikeyan K.T., Nithya A. and Jothivenkatachalam K . , Photocatalytic and antimicrobial activities of chitosan-TiO2 nanocomposite. *Int. J. Biol. Macromol.*, **104,** 1762–1773 (2017).

23. Al-Taweel S. S., Saud H. R., Kadhum A. A. H. and Takriff M. S. , The influence of titanium dioxide nanofiller ratio on morphology and surface properties of TiO2/chitosan nanocomposite. *Results Phys.*, **13,** 102296 (2019).

24. Mahmoud M. E., Ali S. A. A. A. and Elweshahy S. M. T. , Microwave functionalization of titanium oxide nanoparticles with chitosan nanolayer for instantaneous microwave sorption of Cu (II) and Cd (II) from water. *Int. J. Biol. Macromol.*, **111,** 393–399 (2018).

25. Li B., Zhang Y., Yang Y., Qiu W., *et al.* , Synthesis, characterization, and antibacterial activity of chitosan/TiO2 nanocomposite against Xanthomonas oryzae pv. oryzae. *Carbohydr. Polym.*, **152,** 825–831 (2016).

26. Huang K . S., Grumezescu A. M., Chang C. Y., Yang C. H. and Wang, C. Y. , Immobilization and stabilization of TiO2 Nanoparticles in alkaline-solidificated chitosan spheres without cross-linking agent. *Int. J. Latest Res. Sci. Technol.*, **3,** 174–178 (2014).

27. Mahmoud M. E., Ali S. A. A. A., Nassar A. M. G., Elweshahy S. M. T. and Ahmed S. B. , Immobilization of chitosan nanolayers on the surface of nano-titanium oxide as a novel nanocomposite for efficient removal of La (III) from water. *Int. J. Biol. Macromol.*, **101,** 230–240 (2017).

28. Razzaz A., Ghorban S., Hosayni L., Irani M. and Aliabadi M. , Chitosan nanofibers functionalized by TiO2 nanoparticles for the removal of heavy metal ions. *J. Taiwan Inst. Chem. Eng.*, **58,** 333–343 (2016).

29. Huang Q., Jiao Z., Li M., Qiu D., *et al.* , Preparation, characterization, antifungal activity, and mechanism of chitosan/TiO2 hybrid film against bipolaris maydis. *J. Appl. Polym. Sci.*, **128,** 2623–2629 (2013).

30. Beranek R. , (Photo) electrochemical methods for the determination of the band edge positions of TiO2-based nanomaterials. *Adv. Phys. Chem.*, **2011,** (2011).

31. Shi F., Shang D. and Wang Z. , An rGQD/chitosan nanocomposite-based pH-sensitive probe: application to sensing in urease activity assays. *New J. Chem.*, **43,** 13398–13407 (2019).

32. Vlasova N. N. and Markitan O. V. , Surface Complexation Modeling of Biomolecule Adsorptions onto Titania. *Colloids and Interfaces*, **3,** 28 (2019).

33. Blesa M. A., Weisz A. D., Morando P. J., Salfity J. A., *et al.* , The interaction of metal oxide surfaces with complexing agents dissolved in water. **196,** 31–63 (2000).

34. Haldorai Y. and Shim J.-J. , Chitosan-Zinc Oxide hybrid composite for enhanced dye degradation and antibacterial activity. *Compos. Interfaces*, **20,** 365–377 (2013).

35. Youssef A. M., Abou-yousef H., El-sayed S. M. and Kamel, S. , International Journal of Biological Macromolecules Mechanical and antibacterial properties of novel high performance chitosan / nanocomposite films. *Int. J. Biol. Macromol.*, **76,** 25–32 (2015).

36. Patale R. L. and Patravale V. B. , O , N-carboxymethyl chitosan – zinc complex : A novel chitosan complex with enhanced antimicrobial activity. *Carbohydr. Polym.*, **85,** 105–110 (2011).

37. Alagumuthu G. and Kumar T. A. , Synthesis and Characterization of Chitosan / TiO 2 Nanocomposites Using Liquid Phase Deposition Technique. *J. Nanosci.Nanotechnol.,* **4,** 105–111 (2013).

38. Hanna A. A., Mohamed W. A. A. and Ibrahim I.A. , Studies on Photodegradation of Methylene Blue (MB) by Nano-sized Titanium Oxide. *Egypt. J. Chem*, **57,** 315-325 (2014).

39. Marschall R. and Wang L. , Non-metal doping of transition metal oxides for visible-light photocatalysis. *Catal. Today*, **225,** 111–135 (2014).